Cathodic corrosion of Cu substrates as a route to nanostructured Cu/M (M = Ag, Au, Pd) surfaces

Ilija Najdovski,[a] PR Selvakannan[a] and Anthony P. O'Mullane*[a,b]

Abstract: The electrochemical formation of nanostructured materials is generally achieved by reduction of a metal salt onto a substrate that does not influence the composition of the deposit. In this work we report that Ag, Au and Pd electrodeposited onto Cu under conditions where galvanic replacement is not viable and hydrogen gas is evolved results in the formation of nanostructured surfaces that unexpectedly incorporate a high concentration of Cu in the final material. Under cathodic polarization conditions the electrodissolution/corrosion of Cu occurs which provides a source of ionic copper that is reduced at the surface-electrolyte interface. The nanostructured Cu/M (M = Ag, Au and Pd) surfaces are investigated for their catalytic activity for the reduction of 4-nitrophenol by $NaBH_4$ where Cu/Ag was found to be extremely active. This work indicates that a substrate electrode can be utilized in an interesting manner to make bimetallic nanostructures with enhanced catalytic activity.

Introduction

The electrodeposition of metallic nanostructures is a burgeoning research field that offers control over surface morphology, composition, orientation of exposed crystal facets and active sites through a relatively simple process. The basic principle is reducing a metal salt to its metallic form at a conducting electrode where the aforementioned properties are controlled via the deposition protocol which can include the applied potential/current, plating additives, physical templates, solvent, time and temperature.[1] In the vast majority of cases the underlying working electrode merely acts as a surface for the nucleation and growth of the depositing metal with a degree of influence over the morphology of the final material.[2] Interestingly recent studies have shown that under more exertive cathodic polarisation conditions than usually employed for metal deposition very unusual behaviour can be observed at metallic electrodes. Koper reported that metal (Pt, Au, Cu, Ag, Ni, Rh, Si, Nb and Ru) electrodes polarised at -10 V vs reference hydrogen electrode (RHE) results in the formation of fine nanoparticles of that metal at the surface via the formation of Zintl type phases (cation stabilised metal anions) which are reduced to the metallic form when contacted with water once they are exposed beyond the hydrogen gas layer created during such a vigorous protocol.[3] Mirkin demonstrated that Pt polarised at milder conditions of -1.0 V vs Ag/AgCl in 0.1 M KCl containing oxygen resulted in dissolution of Pt.[4] Kreizer and co-workers reported that copper dissolution occurs under even milder cathodic polarisation conditions (-0.40 to -0.70 V vs standard hydrogen electrode (SHE)) in acidic solution in the presence of trace oxygen which is promoted by stirring of the electrode/interface layer by bubbles of evolving hydrogen.[5] In that instance, two competing processes are witnessed; namely the evolution of hydrogen gas together with the re-deposition of the dissolved Cu[5a]. Therefore in this work the electrodeposition of metals such as Ag, Au and Pd on to Cu are investigated under cathodic polarisation conditions where hydrogen gas evolution occurs. Unexpectedly the resultant nanostructured deposit does not consist solely of the depositing metal but a significant amount of Cu is also present. Advantage is taken of this phenomenon to create bimetallic nanostructured surfaces that are highly active for the catalytic reduction of nitrophenol to aminophenol.

Results and Discussion

The electrodeposition of Cu under conditions of hydrogen gas evolution generally results in the formation of highly porous materials where the hydrogen gas bubbles act as a dynamic template over which the metal deposits.[2a, 6] However in those studies the substrate of interest was generally copper and therefore any dissolution that may have occurred would not have been detected or have any significant influence on the process. In this work when Ag is galvanostatically deposited onto Cu from a plating bath consisting of 50 mM $AgNO_3$ in 1.5 M H_2SO_4 at -3 A cm^{-2} for 15 s, which are typical conditions for the formation of porous Cu, a porous structure is formed as expected (Figure 1A). This is also highly comparable to the case where porous Ag is electrodeposited under dynamic hydrogen bubble templating conditions on Pt electrodes.[7] However upon analysis of the material using atomic absorption spectroscopy (AAS) it was found that it contained 60 % Cu even though a copper salt was not present in the electrolyte and the experiment was conducted immediately upon immersion of the copper electrode in the plating bath. XPS analysis confirmed that Cu was also present on the surface of the material. Given this highly surprising result the experiment was repeated using 50 mM $KAuBr_4$ and 50 mM $Pd(NO_3)_2$. As in the case of Ag deposition highly porous deposits were formed for Au (Figure 1C) and Pd (Figure 1E). Upon AAS analysis it was found that the Au and Pd based materials contained 35 % and 56 % Cu respectively. XPS also confirmed that Cu was present on the surface of both deposits. Therefore the effect of incorporating Cu into the final material is the same

[a] Dr. I. Najdovski, Dr. PR Selvakannan, Dr. A. P. O'Mullane
School of Applied Sciences
RMIT University
GPO Box 2476V, Melbourne, VIC 3001, Australia
[b] Current address: Dr. A. P. O'Mullane
School of Chemistry. Physics and Mechanical Engineering
Queensland University of Technology
GPO Box 2434, Brisbane, QLD 4001, Australia
Email: anthony.omullane@qut.edu.au

Supporting information for this article is given via a link at the end of the document.

in all cases, however the identity of the depositing metal affects the pore sizes and internal wall structure as shown when comparing Figures 1 B, D, F.

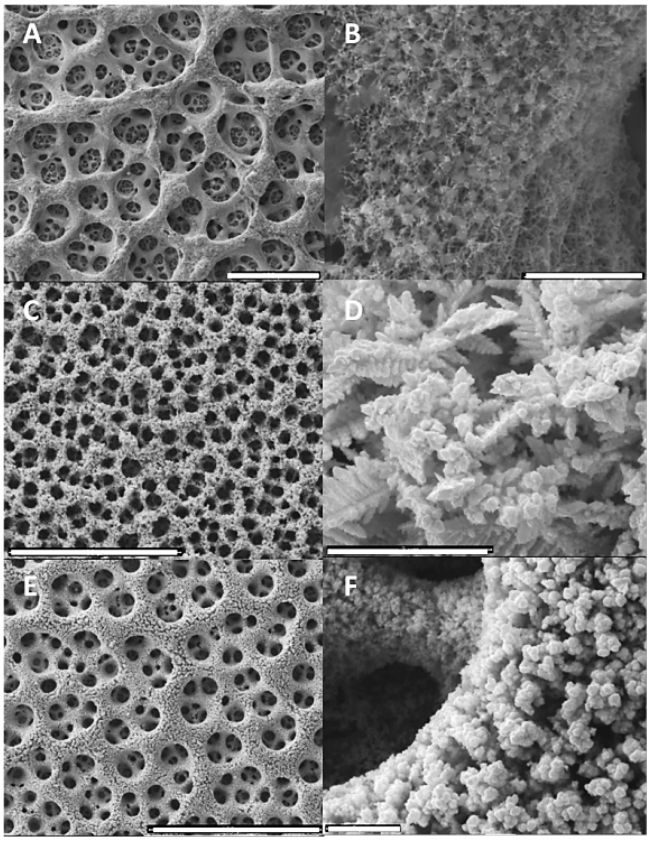

Figure 1. SEM images for electrodeposited (A,B) Ag, (C,D) Au and (E,F) Pd on a copper electrode at – 3 A cm^{-2} for 15 s from a solution of 1.5 M H_2SO_4 containing either 50 mM $AgNO_3$, $KAuBr_4$ or $Pd(NO_3)_2$. Scale bar is 100 µm (left column) and 3 µm (right column).

The difference in morphology can be explained by how hydrogen evolves from the surface which can be monitored via chronopotentiometry (Figure 2). To maintain an applied current density of -3 A cm^{-2} each system attains a potential value far negative of the standard reduction potential for each metal salt and therefore the same amount of hydrogen is assumed to be evolved in each case. The potential value is most negative for Ag and becomes less negative for Au and less negative again for Pd as expected when the exchange current density for hydrogen evolution at Ag, Au and Pd is considered to be a considerable factor in the deposition of these materials[8]. The spiky nature of the data is indicative of hydrogen bubble formation, growth and detachment from the growing deposit[2a]. Clearly the width of each event is largest in the Ag case and indicates significant coalescence of hydrogen bubbles which is reflected in the much larger pore sizes seen for Cu/Ag (Figure 1). Figure S1 shows XRD data for each sample which clearly indicates the formation of metallic Ag, Au and Pd. The peak positions do not suggest alloy formation and each material therefore consists of separated metals that would be in intimate contact with each other and could offer interesting properties for catalytic applications which is discussed below.

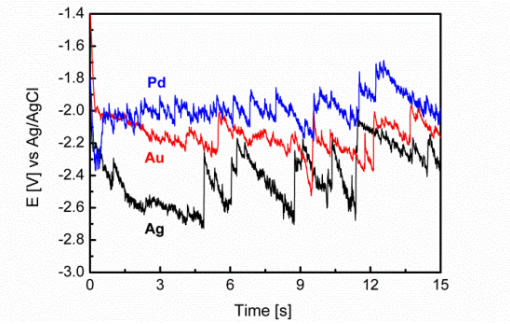

Figure 2. Chronopotentiograms for the deposition of Ag, Au and Pd on to a copper electrode at – 3 A cm^{-2} from a solution of 1.5 M H_2SO_4 containing either 50 mM $AgNO_3$, $KAuBr_4$ or $Pd(NO_3)_2$.

Significantly a cyclic voltammogram recorded for the Pd based sample recorded in 1 M NaOH was indicative of Cu rather than Pd (Figure 3). It is clear from this data that there are no immediately obvious features from Pd, such as the hydrogen absorption/desorption region from -0.90 to -0.60 V (Figure 3C), in the CV for Cu/Pd which is very similar to the CV recorded for porous copper electrodeposited on copper (Figure 3B). Any oxide formation/reduction features of Pd are masked by the formation of copper oxide on the positive sweep and the reduction of these oxides on the reverse sweep from -0.50 to -1.25 V. However the profile for oxide reduction on Cu compared to Cu/Pd is different and indicates that the latter it is not a pure Cu surface. Interestingly, the magnitude of the response was also greater (ca. x 7 times when the oxide formation region is analysed) than a comparable porous Cu sample or considerable greater than a porous Pd sample (electrodeposited on GC) indicating that this approach creates a higher surface area material than deposition of the individual metal under similar conditions. Also, the greater negative current at the beginning of the positive sweep in Figure 3(a) could be attributed to the HER which is absent in Figure 3(b).

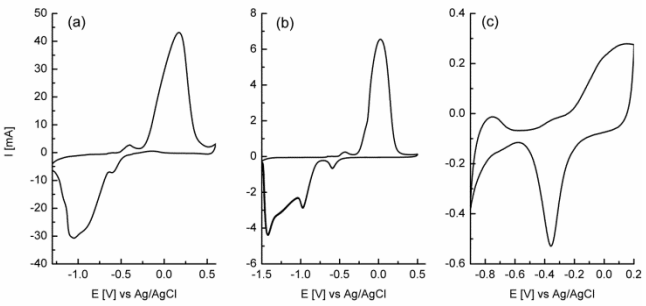

Figure 3: Cyclic voltammograms recorded in 1 M NaOH at (a) Cu/Pd (-3 A cm^{-2} from a solution of 1.5 M H_2SO_4 and 50 mM $Pd(NO_3)_2$), (b) Cu (-3 A cm^{-2} from a solution of 1.5 M H_2SO_4 and 400 mM $CuSO_4$) and (c) Pd (-3 A cm^{-2} for 30 s on a GC electrode from a solution containing 20 mM $Pd(NO_3)_2$ in 1.5 M H_2SO_4.

XPS also confirms the presence of metallic Ag, Au and Pd on the surface (Figure 4) without any indication of alloy formation as evidenced by the XRD data (Figure S1).

However, this raises the question as to what is the source of such a high concentration of Cu in the samples? The galvanic replacement of Cu with the more noble metals can be ruled out as the potential attained by the system is ca. -2.5 V (Figure 2) which is far negative of the standard reduction potential of $Cu^{2+/0}$ (0.34 V vs SHE). Indeed recent studies showed that galvanic replacement does not occur when Pt is electroplated on Cu nanowires[9] or Ni films[10] at potentials more negative than the standard reduction potentials for the $Cu^{2+/0}$ and $Ni^{2+/0}$ couples respectively. It must be noted that in those reports the evolution of hydrogen was not involved. However, according to the studies of Kreizer[5, 11], Cu can be electrochemically dissolved under cathodic polarisation conditions, which is promoted when the electrode/electrolyte layer is perturbed by hydrogen evolution. However for corrosion to occur Cu must still be oxidised, which is facilitated by the presence of trace oxygen. Therefore previous investigations[5, 11] have proposed that $Cu_xO_{x/2(ads)}$ type oxides are formed on the surface which can dissolve in acidic media to generate $Cu^{+}_{(ads)}$ which can be oxidised to $Cu^{2+}_{(ads)}$ in the presence of O_2. Under cathodic polarisation conditions this oxidised Cu can be reduced to the metallic form ($Cu_{(s)}$) or diffuse to the bulk as $Cu^{2+}_{(aq)}$, if there is a very low concentration of crystallisation sites. However, once these sites are established $Cu^{2+}_{(aq)}$ ions diffuse to the surface and are reduced. For each of the systems under study here the composition of the electrolyte was checked pre- and post the electrodeposition experiments by AAS and no evidence of copper was found in the solution indicating that the process was confined to $Cu^{2+}_{(ads)}$ reduction or that any $Cu^{2+}_{(aq)}$ ions that may have been formed were reduced at the surface. The latter is not too surprising in the context of Kreizer's work as metals electrodeposited using the approach reported here are very rough (Figure 1) and therefore contain numerous nucleation sites where Cu deposition would occur.

However it should also be considered that under conditions of vigorous hydrogen gas evolution there will be a significant consumption of protons at the electrode/electrolyte interface and therefore the local pH will be significantly higher than the bulk electrolyte. Given that copper oxides are stable in neutral and alkaline solutions such an electrodissolution mechanism would favour the formation of copper oxides on the deposit. This is the case here as the XRD data in Figure S1 gives clear evidence for the formation of Cu_2O in the Ag and Pd samples and less so in the Au samples. Indeed for porous Cu electrodeposited on Cu the formation of Cu_2O was also reported[12]. Notably the unmodified Cu substrate does not indicate any Cu_2O formation when analysed by XRD which was undertaken in the same timeframe as the electrodeposited samples and therefore the detection of Cu_2O at the porous samples is not simply due to exposure to the atmosphere. This was further confirmed by XPS where Figure 4 shows the Cu 2p core level spectra for each sample where binding energy values for the Au sample (932.5 eV) and Pd and Ag samples (933.0 eV) are indicative of Cu_2O formation.[13] This is more clearly seen from the O1s core level spectra (Figure S2) where the peaks associated with Cu_2O, $Cu(OH)_2$ and mixed oxide phases, and adsorbed hydroxide ions are labelled in the de-convoluted spectra. The satellite peaks in the Cu 2p spectra are quite noticeable and are caused by cupric oxide which has a $3d^9$ configuration and is known to form such shake up satellite peaks[14]. CuO peaks were not seen in the XRD patterns (Figure S1) which indicates that this surface oxide is very thin. Therefore during the course of cathodic polarisation conditions there is clear evidence of Cu oxidation which would provide the source of ionic copper required for its subsequent reduction to the metallic state under potential control. The fact that residual oxides remain on the surface after the experiment indicates that this process must be quite extensive and therefore facilitates such high bulk concentrations of Cu within the Ag, Au and Pd samples. The slightly greater amount of Pd and Au in the samples compared to Ag may be related to the miscibility of the metals where it is known that Cu is highly miscible with Pd[15], Au[16] and almost totally immiscible with Ag[17].

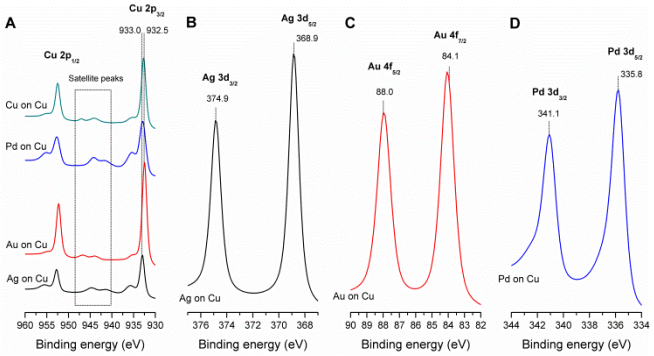

Figure 4. XPS (A) of Cu 2p, (B) Ag 3d, (C) Au 4f and (D) Pd 3d core levels for the samples prepared as in Figure 1.

Table 1. Composition and sizes of Ag, Au and Pd based materials electrodeposited onto Cu substrates. Pore sizes were calculated by analysing SEM images of the materials, bulk mol% was calculated from the data obtained by AAS measurements and the crystallite sizes were determined by analysing the width of the (111) peak for each metal and using the Scherrer equation.

	Cu - Ag	Cu - Au	Cu - Pd
Bulk mol%	61 – 39	35 – 65	56 – 44
Pore size (μm)	63	9	19
Crystallite size (nm)	24 – 23	36 – 33	11 – 26

Surface enhanced Raman spectroscopy (SERS) is a highly surface sensitive technique that is affected by the composition and morphology of the substrate. Therefore, Rhodamine B was immobilised on the surface of each sample and tested for its SERS response (Figure 5A). Clearly the nature of the deposited metal has a significant effect. The relatively non-active Pd results in a dramatic decrease in the SERS response compared to porous Cu only. Interestingly the deposition of SERS active Au does not improve performance over Cu only but using Ag shows a dramatic improvement in the response. The surface

plasmon resonance (SPR) effect can be discounted as the laser used was 785 nm which is well removed from the SPR features of Ag and Au and therefore can be attributed to morphology effects. The internal wall structure of Cu/Ag shows a network of block like crystallites and narrow nanowires throughout the sample that would be the source of many hotspots (areas with higher electromagnetic field due to nanosized features but also the sandwich effect) over the surface. In contrast quite large dendrites are formed for the Cu/Au sample (Figure 1D) which would decrease the available number of hot spots.

The hydrogen evolution reaction is also a powerful probe to characterise sample composition and linear sweep voltammograms for the evolution of hydrogen from Cu/M (M= Ag, Au and Pd) are shown in Figure 5B. As expected the trend in activity in terms of current magnitude and earlier onset potential is CuAg < Cu < Cu/Au < CuPd due to the relevant ability of the metals for this reaction[2a] as well as the increased surface area of Cu/M compared to Cu only. It should be noted that the data for porous Cu only as a comparison required a significantly higher concentration of copper salt (400 mM $CuSO_4$) in the plating bath to achieve the type of structures seen in Figure 1.

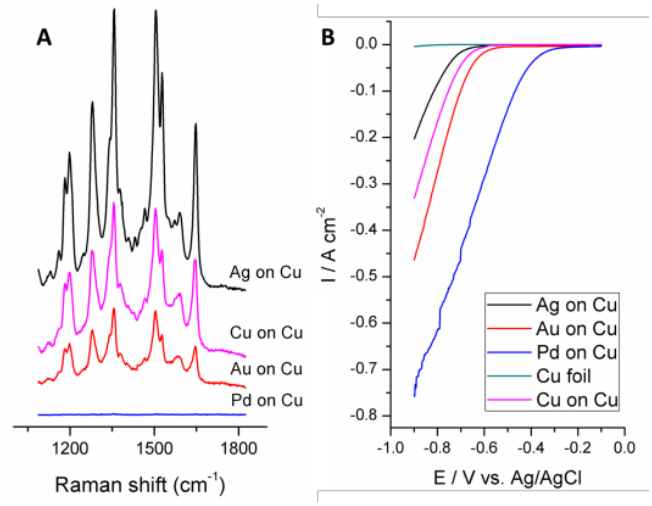

Figure 5. (A) SERS spectra for immobilised Rhodamine B and (B) HER on Cu, Ag, Au and Pd samples prepared as in Figure 1.

The samples were tested for their efficiency towards the reduction of 4-nitrophenol to 4-aminophenol in the presence of excess $NaBH_4$. This reaction can be monitored by UV-vis spectroscopy where the nitrophenolate ion is generated by reaction of nitrophenol with $NaBH_4$ and absorbs strongly at ca. 425 nm (Figure S3). This reaction is thermodynamically feasible, however it is kinetically limited and requires the presence of a catalyst[18]. Ag, Au and Pd nanomaterials have been investigated as catalysts towards this reaction[18a, 19] and our previous work has shown that Cu/Au and Cu/Ag materials are also applicable for this reaction which is beneficial as Cu is a much cheaper material than the more expensive noble metals[12, 20]. Figure 6 displays kinetics data for the reduction of nitrophenol to aminophenol at Cu/Ag, Cu/Au and Cu/Pd. The reaction rates can be calculated by determining the slope of the linear part of the graph (assuming first order kinetics given the excess concentration of $NaBH_4$ used). Large differences in reaction rates can be seen between the 3 samples; Cu/Pd (2.4 x 10^{-4} s^{-1}), Cu/Au (1.4 x 10^{-3} s^{-1}) and Ag (1.6 x 10^{-2} s^{-1}) on Cu. The Cu/Au system was used to compare to the single metallic case, i.e. porous Au. The latter was achieved using a similar deposition protocol from a solution containing 0.1 M $KAuBr_4$ in 1.5 M H_2SO_4 at a current density of – 2 A cm^{-2} for 30 s on a gold substrate to achieve the type of morphology seen for the samples in this study as reported previously[21]. For the catalytic reduction of nitrophenol, a rate of 2.3 x 10^{-4} s^{-1} was determined (Figure S4A) which is inferior to the Cu/Au system (1.4 x 10^{-3} s^{-1}) illustrating the effectiveness of a bimetallic system for this heterogeneous catalytic reaction. For the SERS experiment the Cu/Au system was significantly inferior (Figure S4B) which is not unexpected as Cu is far less SERS active than Au. Similarly for the HER Cu/Au was less active compared to porous Au (Figure S4C) which is also expected given that Cu does not possess good activity for this reaction, in particular when compared to Au.

The low catalytic activity for the Cu/Pd system, even though it possesses the smallest crystallite sizes (Table 1), can be explained because the reduction of nitrophenol is heavily influenced by the adsorption of H on the catalyst surface to initiate electron transfer between $NaBH_4$ and nitrophenol through the catalyst followed by the release of both H and the aminophenol[22]. The strong adsorption of H to Pd would imply a slower turn over frequency due to the delayed release of H from the catalyst's surface. The Cu/Ag system takes advantage of a localised change to the electronic structure as the metals have the same electronegativity but different work functions[23]. This results in electron transfer from Cu to Ag which increases electron density at the silver sites which benefits the hydrogenation of the electron withdrawing nitro group[23]. To further determine the influence of composition on the Cu/Ag catalytic system, 2.5 mM $CuSO_4$ was added to the deposition bath (1.5 M H_2SO_4 and 50 mM $AgNO_3$). The performance of the catalyst is seen to increase dramatically with a small addition of $CuSO_4$ to the plating bath and a reaction rate of 8.5 x 10^{-2} s^{-1} (5.1 min^{-1}) was calculated for this sample. To the best of our knowledge this is one of the highest reaction rates ever reported for this catalytic reaction. Previous studies[23] using a colloidal solution of nano-dumbbells of Cu/Ag gave a reaction rate of 0.498 min^{-1}. The advantage of this system is that the catalyst can be simply recovered from the solution rather than requiring centrifugation to remove the catalyst. The morphological changes between the samples are shown in Figure S5. The changes are subtle and a needle-like dendritic structure is maintained, however they appear longer and slightly more branched for the modified Cu/Ag sample. The XRD (Figure S6) spectra displayed only minor differences with a slight increase in the amount of Cu_2O at the new sample. The bulk composition however did change where the amount of Cu increased from 61 to 77 % as expected when Cu ions are added to the plating bath. Interestingly the SERS response for this sample was also markedly improved (Figure S7) indicating more electromagnetic hotspots which are likely to be the correlated with the enhanced catalytic activity that is seen for this sample. This is the optimised result and other concentrations of $CuSO_4$ (0.625 –

6.25 mM) were tried in all electrolyte solutions for the deposition of Cu/Ag, Cu/Au and Cu/Pd using this approach but a higher catalytic rate for the reduction of nitrophenol was not achieved.

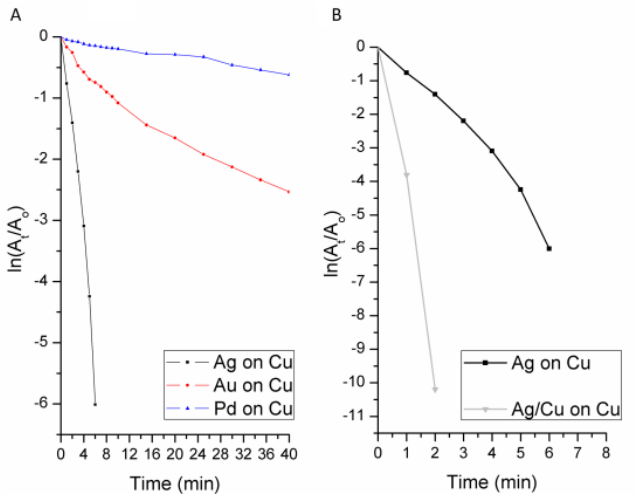

Figure 6. Plot of $\ln(A_t/A_0)$ versus Time for the reduction of 4-nitrophenol by $NaBH_4$ at (A) Ag, Au and Pd samples on Cu and (B) Ag on Cu and Ag on Cu when copper salt was added to the plating bath.

In summary we have reported an unexpected phenomenon during the course of electrodeposition of metals onto a Cu electrode whereby corrosion of the substrate occurs rather than a galvanic replacement process which results in the incorporation of a significant concentration of Cu in the final Cu/Ag, Cu./Au and Cu/Pd materials. These nanostructured bimetallic surfaces were active for nitrophenol reduction to aminophenol with the Cu/Ag sample in particular being highly active. This work also demonstrates that if distinct layers of a more noble metal on a less noble metal are required by electroplating then suppression of the galvanic replacement process by the applied potential is not the only factor involved and that corrosion of the substrate should also be considered.

Experimental Section

Solutions containing $CuSO_4$, $AgNO_3$, H_2SO_4 (Ajax Finechem), rhodamine B (Merck), $KAuBr_4$, $NaBH_4$, NaOH (Sigma Aldrich), $Pd(NO_3)_2$ and 4-nitrophenol (BDH) were used as received and made up with deionized water (resistivity of 18.2 MΩ cm) purified by use of a Milli-Q reagent deioniser (Millipore). Electrochemical experiments were conducted at (20 ± 2) ˚C with a CH Instruments (CHI 760C) electrochemical analyser. A copper foil (0.158 cm^2 area; 99.999% purity purchased from Goodfellow) was used as the working electrode, which was first immersed in diluted HNO_3 (10% v/v) to remove any surface oxides and then washed with acetone and methanol followed by drying in a stream of nitrogen gas prior to use. The reference electrode was Ag/AgCl (3M KCl). For electrodeposition of Cu/M (M = Ag, Au, Pd), an inert graphite rod (3 mm diameter, Johnson Matthey Ultra "F" purity grade) was used as the counter electrode to avoid any possible contaminants from electrodissolution.[24] All electrochemical measurements commenced after degassing for 10 min the electrolyte solutions with nitrogen prior to any measurement. Current density is reported taking the geometric area of the sample into account. SEM measurements were performed on an FEI Nova SEM instrument. XRD measurements were carried out on a Bruker AXS X-ray diffraction system operating at a voltage of 40 kV and current of 40 mA with CuKα radiation. XPS measurements were carried out with a Thermo K-Alpha XPS instrument at a pressure better than $1x10^{-9}$ torr with core levels aligned with the C 1s binding energy of 285 eV. Atomic absorption spectroscopy was done with a Varian AAS spectrophotometer. SERS activity was measured by using a Perkin–Elmer RamanStation 400 operated at an excitation wavelength of 785 nm after immersing the samples in an aqueous 1 mM solution of rhodamine B for 1 h before the unbound rhodamine B was washed off with MilliQ water. The reaction of 1 mM 4-nitrophenol (NP) with 0.1 M $NaBH_4$ was carried out in a 100 ml beaker containing a total volume of 30 ml under stirring conditions (stirrer bar rotated at 800 rpm) with the sample fixed in the solution. The progress of the reaction was monitored by taking aliquots from the reaction mixture and performing UV-visible spectroscopy using a Varian (Cary 50) in a cuvette of 1 cm path length.

Acknowledgements

AOM gratefully acknowledges funding through a Future Fellowship from the Australian Research Council (FT110100760). The authors acknowledge the facilities, and the scientific and technical assistance, of the Australian Microscopy and Microanalysis Research Facility at the RMIT Microscopy & Microanalysis Facility.

Keywords: electrodeposition • corrosion • catalysis • nanostructures • bimetallic

[1] a) A. P. O'Mullane, *Nanoscale* **2014**, *6*, 4012-4026; b) B. J. Plowman, S. K. Bhargava, A. P. O'Mullane, *Analyst* **2011**, *136*, 5107-5119; c) *Electrodeposition, Theory and Practice*, Springer, **2010**; d) F. Ye, L. Chen, J. Li, J. Li, X. Wang, *Electrochem. Commun.* **2008**, *10*, 476-479; e) L. P. Bicelli, B. Bozzini, C. Mele, L. D'Urzo, *Int. J. Electrochem. Sci.* **2008**, *4*, 356-527; f) J.-H. Kim, R.-H. Kim, H.-S. Kwon, *Electrochem. Commun.* **2008**, *10*, 1148-1151; g) F. Endres, D. MacFarlane, A. Abbott, *Electrodeposition from Ionic Liquids*, Wiley - VCH, Weinheim, **2008**; h) B. J. Plowman, A. P. O'Mullane, S. K. Bhargava, *Faraday Discuss.* **2011**, *152*, 43-62.

[2] a) I. Najdovski, A. P. O'Mullane, *J. Electroanal. Chem.* **2014**, *722-723*, 95-101; b) F. Ebrahimi, Z. Ahmed, *Mater. Characterisation* **2002**, *49*, 373-379; c) Y. Liu, Y. Liu, R. Mu, H. Yang, C. Shao, J. Zhang, Y. Lu, D. Shen, X. Fan, *Semiconductor science and technology* **2005**, *20*, 44; d) J. Lin-Cai, D. Pletcher, *J. Electroanal. Chem. Interfac. Electrochem.* **1983**, *149*, 237-247.

[3] A. I. Yanson, P. Rodriguez, N. Garcia-Araez, R. V. Mom, F. D. Tichelaar, M. T. M. Koper, *Angew. Chem. Int. Ed.* **2011**, *50*, 6346-6350.

[4] J.-M. Noël, Y. Yu, M. V. Mirkin, *Langmuir* **2013**, *29*, 1346-1350.

[5] a) I. Kreizer, N. Tutukina, I. Zartsyn, I. Marshakov, *Protection of Metals* **2002**, *38*, 226-232; b)V. Kreizer, I. Marshakov, N. Tutukina, I. Zartsyn, *Protection of Metals* **2003**, *39*, 30-33.

[6] a) M. Mahajan, S. K. Bhargava, A. P. O'Mullane, *Electrochim. Acta* **2013**, *101*, 186-195; b) N. D. Nikolić, K. I. Popov, in *Modern Aspects of Electrochemistry, Vol. 48* (Ed.: S. S. Djokic), Springer New York, **2010**, pp. 1-70; c) R. Kim, D. Han, D. Nam, J. Kim, H. Kwon, *J. Electrochem. Soc.* **2010**, *157*, D269-D273; d) S. Cherevko, C.-H. Chung, *Talanta* **2010**, *80*, 1371-1377; e) N. D. Nikolic, G. Brankovic, M. G. Pavlovic, K. I. Popov, *J. Electroanal. Chem.* **2008**, *621*, 13-21; f) N. D. Nikolic, L. J. Pavlovic, M. G. Pavlovic, K. I. Popov, *Electrochim. Acta* **2007**, *52*, 8096-8104; g) N. D. Nikolic, K. I. Popov, L. J. Pavlovic, M. G. Pavlovic, *Surf. Coat. Technol.* **2006**, *201*, 560-566.

[7] S. Cherevko, X. Xing, C.-H. Chung, *Electrochem. Commun.* **2010**, *12*, 467-470.

[8] W. Sheng, M. Myint, J. G. Chen, Y. Yan, *Energy Environ. Sc.* **2013**, *6*, 1509-1512.

[9] Z. Chen, S. Ye, A. R. Wilson, Y.-C. Ha, B. J. Wiley, *Energy Environ. Sc.* **2014**, *7*, 1461-1467.

[10] A. W. Maijenburg, A. George, D. Samal, M. Nijland, R. Besselink, B. Kuiper, J. E. Kleibeuker, J. E. ten Elshof, *Electrochim. Acta* **2012**, *81*, 123-128.

[11] I. Kreizer, I. Marshakov, N. Tutukina, I. Zartsyn, *Protection of Metals* **2004**, *40*, 23-25.

[12] I. Najdovski, P. R. Selvakannan, A. P. O'Mullane, *RSC Adv.* **2014**, *4*, 7207-7215.

[13] a) B. V. Crist, *Handbook of Monochromatic XPS Spectra, The Elements of Native Oxides* XPS International, LLC, California, **1999**; b) Y. Iijima, N. Niimura, K. Hiraoka, *Surf. Interfac. Anal.* **1996**, *24*, 193-197.

[14] G. Ertl, R. Hierl, H. Knözinger, N. Thiele, H. P. Urbach, *Appl. Surf. Sc.* **1980**, *5*, 49-64.

[15] a) J. S. Bradley, E. W. Hill, C. Klein, B. Chaudret, A. Duteil, *Chemistry of Materials* **1993**, *5*, 254-256; b) F. Roa, J. D. Way, R. L. McCormick, S. N. Paglieri, *Chem. Eng. J.* **2003**, *93*, 11-22.

[16] a) V. Ozoliņš, C. Wolverton, A. Zunger, *Phys. Rev. B* **1998**, *57*, 6427-6443; b) S. H. Wei, A. A. Mbaye, L. G. Ferreira, A. Zunger, *Phys. Rev. B* **1987**, *36*, 4163-4185.

[17] a) P. R. Subramanian, J. H. Perepezko, *JPE* **1993**, *14*, 62-75; b) M. K. I. Arafa, *Proc. Phys. Soc. Sec. B* **1949**, *62*, 238.

[18] a) S. Jana, S. K. Ghosh, S. Nath, S. Pande, S. Praharaj, S. Panigrahi, S. Basu, T. Endo, T. Pal, *Appl. Catal. A* **2006**, *313*, 41-48; b) S. Saha, A. Pal, S. Kundu, S. Basu, T. Pal, *Langmuir* **2009**, *26*, 2885-2893.

[19] a) K. Esumi, R. Isono, T. Yoshimura, *Langmuir* **2003**, *20*, 237-243; b) P. Liu, M. Zhao, *Appl. Surf. Sc.* **2009**, *255*, 3989-3993; c) S. Panigrahi, S. Basu, S. Praharaj, S. Pande, S. Jana, A. Pal, S. K. Ghosh, T. Pal, *J. Phys. Chem. C* **2007**, *111*, 4596-4605.

[20] I. Najdovski, P. R. Selvakannan, S. K. Bhargava, A. P. O'Mullane, *Nanoscale* **2012**, *4*, 6298-6306.

[21] B. J. Plowman, A. P. O'Mullane, P. R. Selvakannan, S. K. Bhargava, *Chem. Commun.* **2010**, *46*, 9182-9184.

[22] a) N. Pradhan, A. Pal, T. Pal, *Langmuir* **2001**, *17*, 1800-1802; b) M. J. Vaidya, S. M. Kulkarni, R. V. Chaudhari, *Org. Proc. Res. Develop.* **2003**, *7*, 202-208; c) S. Wunder, F. Polzer, Y. Lu, Y. Mei, M. Ballauff, *J. Phys. Chem. C* **2010**, *114*, 8814-8820.

[23] X. Huang, Y. Li, H. Zhou, X. Zhong, X. Duan, Y. Huang, *Chem. Eur. J.* **2012**, *18*, 9505-9510.

[24] L. D. Burke, A. P. O'Mullane, V. E. Lodge, M. B. Mooney, *J. Solid State Electrochem.* **2001**, *5*, 319-327.

ARTICLE

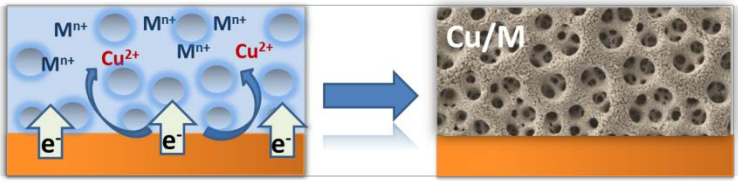

The electrodeposition of Ag, Au or Pd onto a Cu electrode under hydrogen evolution conditions results in the unexpected deposition of Cu within the nanostructured metal deposit. This occurs via the cathodic corrosion of copper which provides a source of copper ions that can be reduced during the deposition process. The morphology of the final porous material and copper content is highly dependent on the metal salt in solution which impacts on the catalytic performance of the material where Cu/Ag was found to be highly active.

*Ilija Najdovski, PR Selvakannan, Anthony P. O'Mullane**

Page No. – Page No.

Electrodeposition of Cu/M (M = Ag, Au, Pd) nanostructured surfaces via the cathodic polarization of Cu substrates